



# Activin-like kinase 5 (ALK5) inactivation in the mouse uterus results in metastatic endometrial carcinoma

Diana Monsivais<sup>a,b,c,1</sup>, Jia Peng<sup>a,c,d,1</sup>, Yibin Kang<sup>d</sup>, and Martin M. Matzuk<sup>a,b,c,e,f,g,h,2</sup>

<sup>a</sup>Department of Pathology and Immunology, Baylor College of Medicine, Houston, TX 77030; <sup>b</sup>Center for Drug Discovery, Baylor College of Medicine, Houston, TX 77030; <sup>c</sup>Center for Reproductive Medicine, Baylor College of Medicine, Houston, TX 77030; <sup>d</sup>Department of Molecular Biology, Princeton University, Princeton, NJ 08544; <sup>e</sup>Department of Molecular and Human Genetics, Baylor College of Medicine, Houston, TX 77030; <sup>f</sup>Department of Molecular and Cellular Biology, Baylor College of Medicine, Houston, TX 77030; <sup>g</sup>Department of Pharmacology and Chemical Biology, Baylor College of Medicine, Houston, TX 77030; and <sup>h</sup>Program in Developmental Biology, Baylor College of Medicine, Houston, TX 77030

Contributed by Martin M. Matzuk, December 6, 2018 (sent for review April 30, 2018; reviewed by Milan K. Bagchi and Thomas E. Spencer)

The endometrial lining of the uterine cavity is a highly dynamic tissue that is under the continuous control of the ovarian steroid hormones, estrogen and progesterone. Endometrial adenocarcinoma arises from the uncontrolled growth of the endometrial glands, which is typically associated with unopposed estrogen action and frequently occurs in older postmenopausal women. The incidence of endometrial cancer among younger women has been rising due to increasing rates of obesity, a major risk factor for the disease. The transforming growth factor  $\beta$  (TGF $\beta$ ) family is a highly conserved group of proteins with roles in cellular differentiation, proliferation, and cancer. Inactivating mutations in the genes encoding the TGF $\beta$  cell surface receptors (*TGFBR1/ALK5* and *TGFBR2*) have been detected in various human cancers, indicating that a functional TGF $\beta$  signaling pathway is required for evading tumorigenesis. In this study, we present a mouse model with conditional inactivation of activin receptor-like kinase 5 (ALK5) in the mouse uterus using progesterone receptor cre ("*Alk5* cKO") that develops endometrial adenocarcinoma with metastasis to the lungs. The cancer and metastatic lung nodules are estrogen dependent and retain estrogen receptor  $\alpha$  (ER $\alpha$ ) reactivity, but have decreased levels of progesterone receptor (PR) protein. The endometrial tumors develop only in *Alk5* cKO mice that are mated to fertile males, indicating that TGF $\beta$ -mediated postpartum endometrial repair is critical for endometrial function. Overall, these studies indicate that TGF $\beta$  signaling through *TGFBR1/ALK5* in the endometrium is required for endometrial homeostasis, tumor suppression, and postpartum endometrial regeneration.

endometrial cancer | knockout mouse | TGF $\beta$  | estrogen receptor

Endometrial cancer is the most common gynecological malignancy in the United States, affecting ~61,380 women and resulting in 10,920 deaths in 2017 (1–3). Endometrial tumors can be broadly categorized into two subtypes (4, 5). Type I endometrial tumors are estrogen dependent, well-differentiated tumors that are associated with obesity and account for the majority (70–80%) of endometrial tumors. Type II endometrial tumors are more common among older postmenopausal women, are more aggressive, hormone independent, and have a less favorable prognosis than type I endometrial tumors. Previous studies indicate that type I endometrial tumors are characterized by mutations in the PI3K/AKT signaling pathway (6–8); whereas mutations in *TP53*, *PIK3CA*, and *PPP2R1A* are commonly observed in type II endometrial tumors (9, 10). The advent of exome sequencing has redefined the classification of endometrial cancers, opening the possibility for targeted therapies that are specific to the molecular aberrations within the tumor. For example, The Cancer Genome Atlas identified mutations in the gene encoding the catalytic unit of DNA polymerase epsilon (*POLE*) that are present in a subtype of endometrial tumors characterized by high mutation rates (11). This type of advanced molecular profiling has resulted in the novel classification of endometrial tumors into four distinct subtypes, providing insight into the signaling aberrations that lead to endometrial tumorigenesis.

The TGF $\beta$  signaling family is composed of highly conserved ligands that transduce signals in an autocrine or paracrine manner through a cell surface heterotetrameric receptor complex

(12, 13). The cell surface receptor complex responding to TGF $\beta$  is composed of the type 1 receptor, *TGFBR1/ALK5*, and the type 2 receptor, *TGFBR2* (14). Upon binding of the ligand, the receptors emit intracellular signals by phosphorylating SMAD2 and SMAD3, which form a complex with SMAD4, and together translocate to the nucleus to control the expression of gene targets (12). Mutations in genes affecting TGF $\beta$  signaling are observed in ovarian, colon, and gastric adenocarcinoma, and in small cell lung carcinoma (15–18). Specifically, the polyadenine repeat in *TGFBR2* is frequently mutated in cancers that are associated with microsatellite instability (19, 20). The inactivated mismatch repair system in microsatellite instability renders the replication machinery susceptible to errors during DNA replication, particularly affecting short DNA sequence repeats, such as those observed in *TGFBR2*. Missense and frameshift *TGFBR1* mutations are also observed in ovarian, esophageal, and head and neck cancers (16, 19, 21). Collectively, these mutations indicate that a functional TGF $\beta$  signaling program is required for cellular homeostasis and may be protective against tumorigenesis.

Studies using mouse models have demonstrated the critical role of the TGF $\beta$  family in reproductive function (22). These studies have revealed that members of the TGF $\beta$  family signaling pathway control diverse roles in reproductive function such as sexual differentiation during embryonic development and in the

## Significance

The rising incidence of endometrial cancer in the United States and worldwide can be partially attributed to elevated rates of obesity in the population. Although hysterectomy is an effective treatment for early endometrial cancer, medical interventions are required in advanced cases with metastatic disease or for women wishing to preserve fertility. Here, we present a mouse model with conditional inactivation of the transforming growth factor  $\beta$  (TGF $\beta$ ) receptor, activin-like kinase 5 (*Alk5*), that develops estrogen-dependent endometrial adenocarcinoma with distant lung metastases. We anticipate that this mouse will be a useful preclinical model for testing novel therapies for endometrial cancer and for understanding the mechanisms that control endometrial regeneration in the postpartum uterus.

Author contributions: D.M., J.P., Y.K., and M.M.M. designed research; D.M. and J.P. performed research; M.M.M. contributed new reagents/analytic tools; D.M., J.P., and M.M.M. analyzed data; and D.M., J.P., and M.M.M. wrote the paper.

Reviewers: M.K.B., University of Illinois; and T.E.S., University of Missouri.

Conflict of interest statement: D.M. and T.E.S. are coauthors on a 2015 Commentary article.

This open access article is distributed under Creative Commons Attribution-NonCommercial-NoDerivatives License 4.0 (CC BY-NC-ND).

See Commentary on page 3367.

<sup>1</sup>D.M. and J.P. contributed equally to this work.

<sup>2</sup>To whom correspondence should be addressed. Email: mmatzuk@bcm.edu.

This article contains supporting information online at [www.pnas.org/lookup/suppl/doi:10.1073/pnas.1806838116/-DCSupplemental](http://www.pnas.org/lookup/suppl/doi:10.1073/pnas.1806838116/-DCSupplemental).

Published online January 17, 2019.

reproductive axis, where TGF $\beta$  family ligands are paramount for the function of the hypothalamic–pituitary–gonadal axis (23, 24). In the female reproductive tract, TGF $\beta$ , its receptor, TGFBR1/ALK5, and its downstream signaling factors, SMAD2 and SMAD3, are critical for the structural integrity of the myometrium and oviducts (25, 26). In fact, conditional ablation of TGFBR1/ALK5 in the uterine muscle and stromal uterine compartments with anti-Müllerian hormone receptor type 2-cre (*Amhr2-cre*) results in abnormal smooth muscle development, leading to oviductal diverticuli and disrupted embryo transport. Alternatively, ablation of TGFBR1/ALK5 from the uterine muscle, stroma, and epithelium with progesterone receptor-cre (*Pgr-cre*) results in endometrial and placental defects, giving rise to abnormal embryo development and infertility (27). Furthermore, it was recently shown that mice with dual conditional deletion of TGFBR1/ALK5 and PTEN using *Pgr-cre* developed endometrial tumors with lung metastases (28).

In this study, we present data that underscore the importance of TGF $\beta$ -mediated signaling to endometrial homeostasis. We describe the development of an estrogen-dependent endometrial adenocarcinoma with lung metastasis that arises in mice with conditional inactivation of TGFBR1/ALK5. Our findings indicate a relationship between estrogen-mediated signaling, the TGF $\beta$  pathway, and the homeostasis of the endometrium.

## Results

**Female Mice with Uterine Inactivation of ALK5 Develop Metastatic Endometrial Tumors.** We previously reported that conditional inactivation of *Tgfr1/Alk5* using progesterone receptor cre (“*Alk5*

cKO”) resulted in female subfertility due to implantation, decidualization, and placental defects (27). After prolonged mating to wild-type (WT) male mice during the fertility studies, we observed that *Alk5* cKO females developed endometrial tumors that metastasized to the lungs. Control and *Alk5* cKO mice were mated continuously to WT males for at least 6 mo beginning at 6 wk of age (Fig. 1 A–C). Interestingly, the endometrial tumors only developed in *Alk5* cKO mice that were mated to fertile males; as virgin mice, mice mated to vasectomized males, or ovariectomized mice treated with estrogen for 3 mo, did not exhibit the endometrial tumor phenotype (*SI Appendix, Table S1*). Over half of the female mice died during the study; however, upon dissection, the cause of death was determined to be related to the reproductive defects and unrelated to the cancers (*SI Appendix, Fig. S1 and Table S1*). Specifically, the mice died from suspected sepsis as indicated by large intrauterine abscesses which formed around a dead fetus (*SI Appendix, Fig. S1*) or due to uterine hemorrhage. This is consistent with our previously reported study (27), which showed mortality of ~40% in the mated *Alk5* cKO mice. Of the mated *Alk5* cKO mice who did not die from pregnancy-related complications, all went on to develop uterine tumors with lung metastasis (*SI Appendix, Table S1*). Because the mothers were also dying prematurely due to problems during pregnancy, it precluded our ability to determine the rate of mortality due to the endometrial tumors and metastases. The experiments presented in this study are intended to define how uterine ALK5 inactivation results in endometrial cancers and lung metastasis.

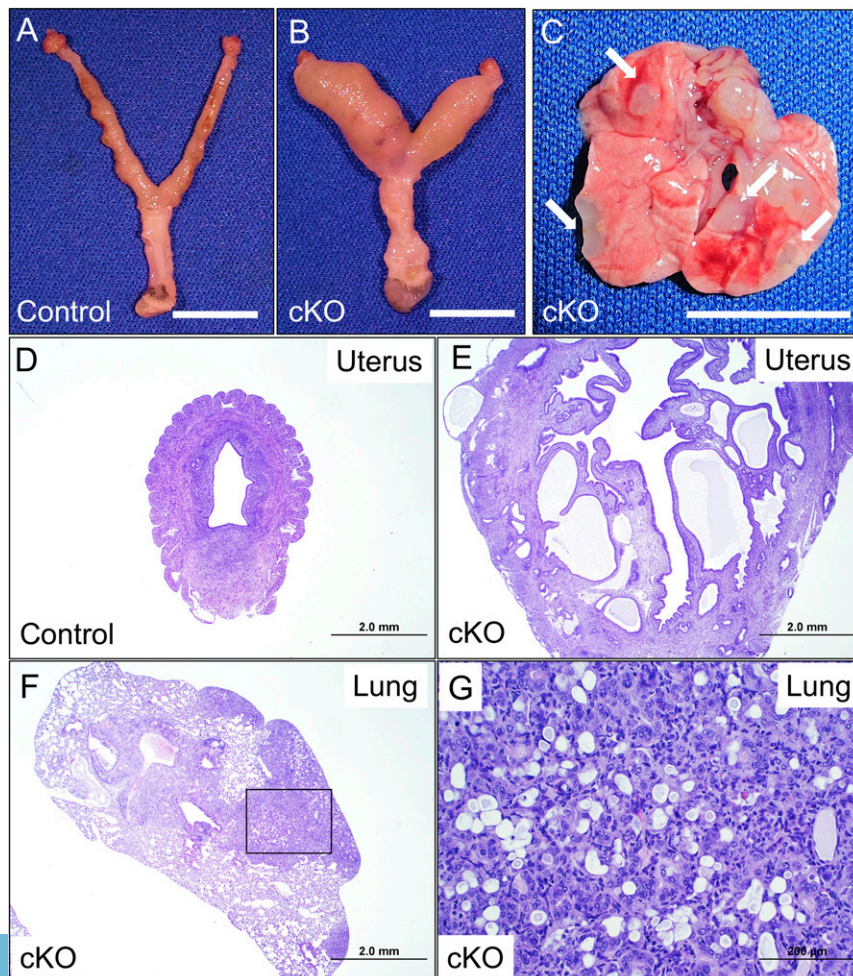


**Fig. 1.** Conditional inactivation of *Alk5* with *Pgr-cre* results in endometrial cancer and lung metastasis. (A and B) Uterus of a control (A) and *Alk5* cKO (B) mouse following 6 mo of continuous mating beginning at 6 wk of age (age 7.5 mo). (C) Lungs and lung metastases from an *Alk5* cKO mouse; white arrows indicate metastatic lung nodules. (Scale bar, 1 cm.) (D and E) H&E stain of a uterine section from a control (D) and from an *Alk5* cKO (E) mouse. (Scale bar, 2 mm.) (F and G) H&E stain of a lung section from an *Alk5* cKO mouse; black box (F) denotes the metastatic lung nodule and area of magnification in G. Mice were collected after being continuously mated to male mice for 6 mo and represent randomly cycling and/or pregnancy states. [Scale bar, 2 mm (F) and 200  $\mu$ m (G).]



Histological examination of the uterus confirmed the presence of endometrial glands within the myometrial layer of the uterus (Fig. 1 *D* and *E*). Hematoxylin and eosin (H&E) staining of the lungs also revealed the presence of invasive glandular tissue in the metastatic lung nodules of *Alk5* cKO females (Fig. 1 *F* and *G*). We used antibody immunostaining to further characterize the cancers in the *Alk5* cKO mice (Fig. 2). Smooth muscle actin (SMA) indicates the myometrial compartment of the uterus and cytokeratin 8 (CK8) specifies the endometrial luminal and glandular epithelium. In the control uterus, the SMA-positive myometrium is an intact layer encapsulating the CK8-positive endometrium (Fig. 2*A*). In contrast, CK8-positive glands have invaded the myometrial layer of the uterus in the *Alk5* cKO mice (Fig. 2*B*). Immunohistochemistry with the glandular epithelium marker, FOXA2, showed that the uterine glands from both control and *Alk5* cKO expressed FOXA2, and that the expression of FOXA2 remained in the endometrial glands that had invaded into the myometrium (SI Appendix, Fig. S2*A* and *B*). To determine the tissue compartment distribution of *Alk5* in the uterus, we quantified *Alk5* expression in the luminal uterine epithelium and in endometrial stromal and myometrial compartments using quantitative real-time PCR. These results indicated that *Alk5* was more highly expressed in the epithelium than in the stromal and myometrial compartments of the uterus ( $10.04 \pm 1.68$  vs.  $1 \pm 0.81$ ,  $P = 0.003$ ) (SI Appendix, Fig. S2*C*).

We observed that in addition to endometrial cancers, the *Alk5* cKO females also developed cervical and vaginal masses. Analysis of these tissues indicated a similar pattern of invasive epithelium in the vaginal and cervical epithelium of the *Alk5* cKO mice (Fig. 2 *C–F*). Cytokeratin 14 (CK14) indicates the intact squamous epithelial layer that is present in the vaginal and cervical epithelium of control mice (Fig. 2 *C* and *E*) (29). In the cervix and epithelium of the *Alk5* cKO mice, this layer of squamous cellular epithelium has been invaded by CK8-positive epithelium (Fig. 2 *D* and *F*). Therefore, defects in the uterus, cervix, and vagina occur after conditional inactivation of ALK5 in the female reproductive tract.

**Estrogen Receptor  $\alpha$  and Progesterone Receptor Expression in the Reproductive Tract of *Alk5* cKO Mice.** The majority of endometrial cancers are estrogen receptor  $\alpha$  (ER $\alpha$ ) and progesterone receptor (PR) positive, and ER $\alpha$ /PR expression is associated with early stage, low grade tumors and more favorable outcomes (2, 5, 30). We performed immunostaining of CK8, PR, and ER $\alpha$  (Fig. 3) in cross-sections of uterine, cervical, and vaginal tissues of control and *Alk5* cKO mice that were mated to WT males for 6 mo beginning at 6 wk of age. As expected, PR protein was readily detected in the epithelial and stromal cells of the endometrium of control mice (Fig. 3*A*). However, PR protein was decreased in the luminal epithelium of the *Alk5* cKO mice but detectable in the stroma (Fig. 3*B*). There were no noticeable differences in PR detection in the cervical or vaginal tissue of the control and *Alk5* cKO mice (Fig. 3 *C–F*). ER $\alpha$  was unchanged in the cervix and vagina of the control and *Alk5* cKO mice (Fig. 3 *I–L*). ER $\alpha$  expression was also present in the endometrial stroma of controls and *Alk5* cKO mice, but its expression was lost in the uterine glands of *Alk5* cKO mice (Fig. 3 *G* and *H*). This suggests that the endometrial tumors in the *Alk5* cKO mice are similar to the hormone-dependent type I endometrial tumors in women (5).

**Three-Dimensional Visualization and Molecular Marker Analysis of the Metastatic Lung Nodules in *Alk5* cKO Mice.** We compared lungs from a normal and *Alk5* cKO mouse using 3D iodine-contrast microcomputed tomography (microCT) analysis. Whereas normal lung architecture is observed in the control lungs, masses (metastatic nodules) are detected in the lungs dissected from *Alk5* cKO mice after mating to WT males for 6 mo (Fig. 4 *A* and *B*). To determine if the origin of these metastatic masses was from the vaginal–cervical or uterine epithelium, cross-sections of the lung tumor metastases were immunostained with the uterine epithelial cell marker, CK8, and the vaginal–cervical squamous cell-epithelial marker, CK14 (Fig. 4*C*). The lung tumor nodules were strongly positive for the epithelial cell marker, CK8, but negative for CK14, indicating that the lung nodules likely metastasized from the endometrial cancers. The metastatic lung

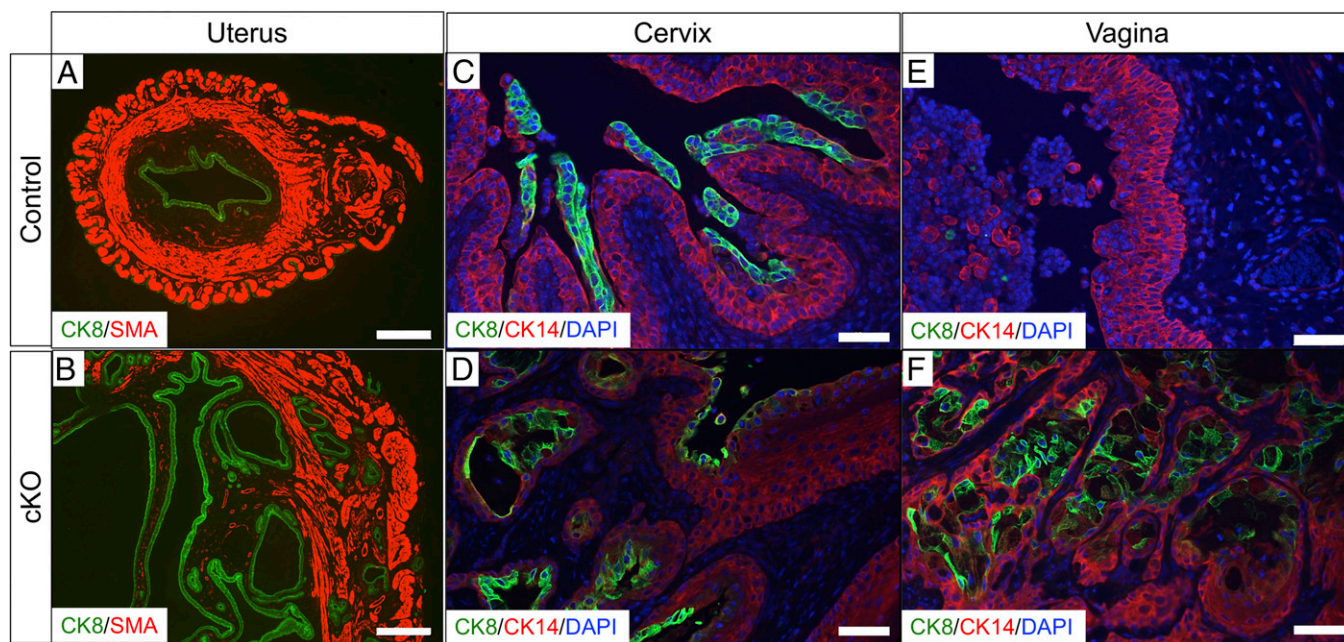


**Fig. 2.** *Alk5* cKO female mice develop cancer in the reproductive tract. (*A* and *B*) Uterine sections stained with the myometrial marker, SMA and the epithelial cell marker, cytokeratin 8 (CK8), from control (*A*) and *Alk5* cKO (*B*) mice. (*C* and *D*) Cervical tissue sections from control (*C*) and *Alk5* cKO (*D*) mice stained with the squamous cell marker, CK14 and CK8. (*E* and *F*) Vaginal tissue sections from control (*E*) and *Alk5* cKO mice (*F*) stained with CK14 and CK8. Tissues were collected from control and *Alk5* cKO mice following 6 mo of continuous mating to WT males. [Scale bar, 500  $\mu$ m (*A* and *B*) and 50  $\mu$ m (*C–F*).]



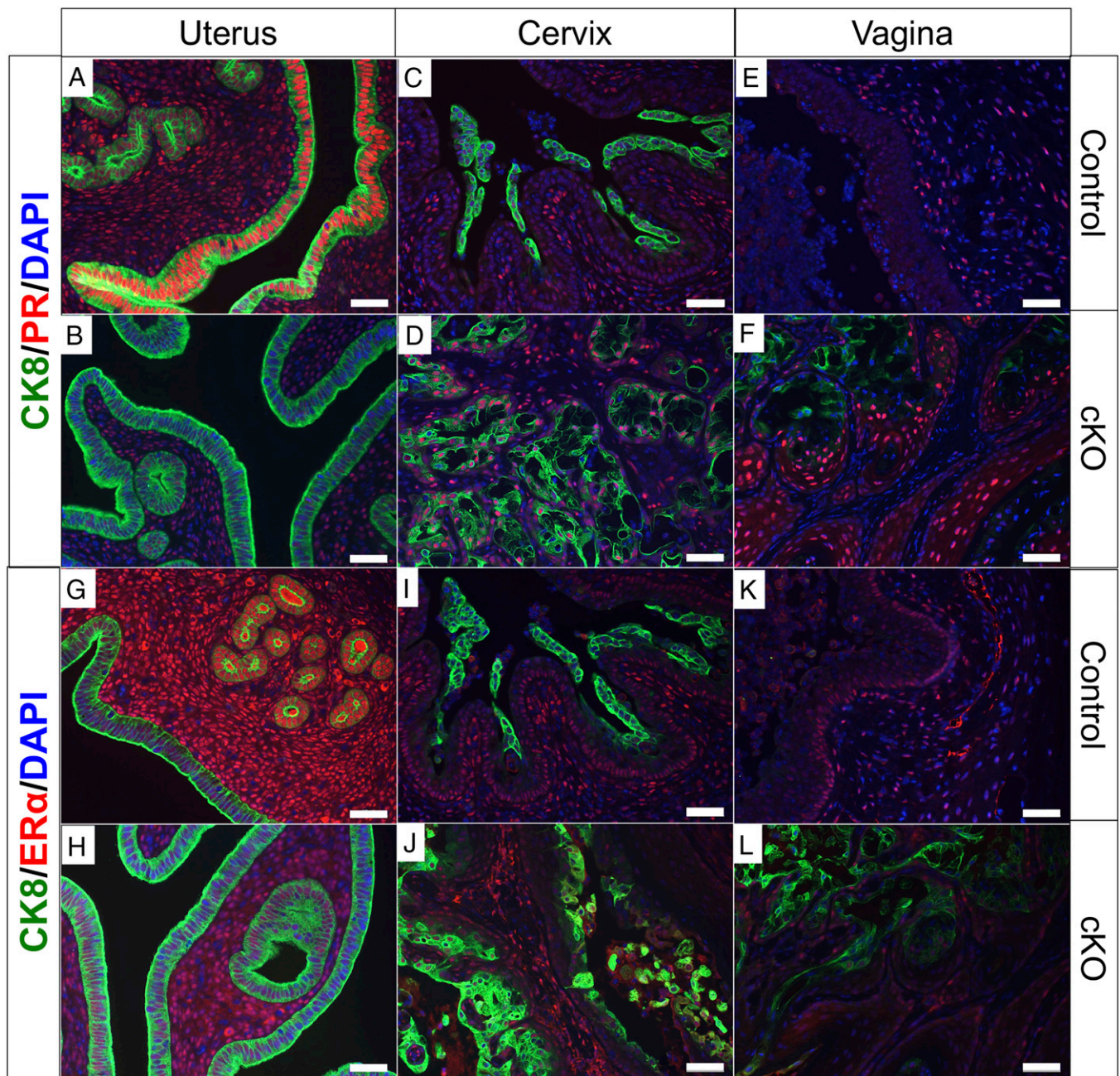


**Fig. 3.** Estrogen receptor  $\alpha$  and progesterone receptor immunostaining. Cross-sections of uterine (A, B, G, and H), cervical (C, D, I, and J), and vaginal tissues (E, F, K, and L) from control (A, C, E, G, I, and K) and *Alk5* cKO (B, D, F, H, J, and L) mice were immunostained with CK8 and PR antibodies (A–F), or with CK8 and ER $\alpha$  antibodies (G–L). Tissues were dissected from mice following 6 mo of continuous mating to male mice. (Scale bar, 50  $\mu$ m.)

nodules were highly proliferative, as observed by the strong immunoreactivity to the proliferation marker, phosphorylated histone H3 (pHH3) (Fig. 4D). We also assessed PR and ER $\alpha$  expression in the lung nodules and determined that while the lung nodules were negative for PR (Fig. 4E), they were positive for ER $\alpha$  (Fig. 4F). Thus, similar to the tissue of origin, the metastatic lung nodules maintained ER $\alpha$  but lost PR protein expression.

#### Lung Metastases Arise from the Uterine Epithelium of *Alk5* cKO Mice.

To examine whether the nodules in the lungs of *Alk5* cKO mice were in fact metastases of uterine origin, we assessed the recombination status of the *Alk5* LoxP sites across various tissues in the *Alk5* cKO mice following 6 mo of mating to WT males

(Fig. 5A). As expected, expression of the floxed *Alk5* allele could be ubiquitously detected in all of the tissues analyzed (Fig. 5B). Although recombination was expected to occur only in the progesterone receptor-expressing tissues (ovary, oviduct, uterus, cervix, and vagina) (31), the lung nodules also expressed the recombinant *Alk5* allele (Fig. 5C). This provided evidence that the lung metastases originated from the reproductive tract. Additional evidence in support of this was obtained by breeding the *Alk5* cKO mice to *Rosa26*<sup>tdTomato</sup> reporter mice. tdTomato expression was obtained in the uterus, ovaries, and oviducts of the reproductive tract and in the metastatic lung nodules of the *Alk5* cKO mice (SI Appendix, Fig. S3 A–D), suggesting that the lung nodules were of gynecologic origin.



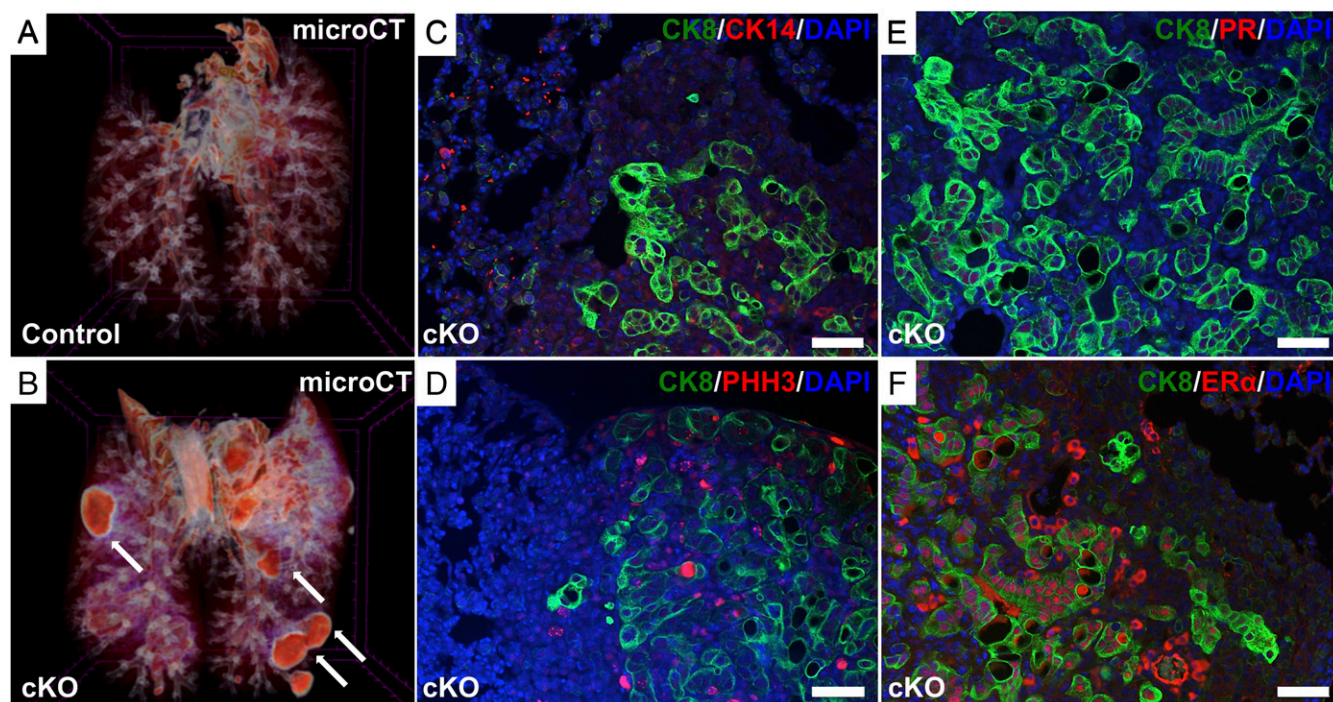


**Fig. 4.** Three-dimensional visualization and immunofluorescence analysis of the lungs reveal metastatic lung nodules in the *Alk5* cKO mice. Micro-CT was performed in the lungs of control (A) and *Alk5* cKO (B) mice after being continuously mated to males for 6 mo beginning at 6 wk of age. White arrows indicate the metastatic lung nodules in the *Alk5* cKO mice (B). Cross-sections of lung tissue with metastatic nodules from the *Alk5* cKO mice were immunostained with CK8 and CK14 (C); CK8 and pHH3 (D); CK8 and PR (E); and CK8 and ER $\alpha$  (F). (Scale bar, 50  $\mu$ m.)

PAX8 is a transcription factor involved in Müllerian tract development that has been used as a marker of malignancies of the reproductive tract (32). PAX8 is particularly useful to assess metastases of gynecologic origin, since its expression is normally absent from the breast, lung, and gastrointestinal tract. PAX8 protein expression was detected in both the uterine glands and lung metastases of the *Alk5* cKO mice (Fig. 5 D and E). In the lungs, the PAX8-positive cells were also positive for CK8 (Fig. 5 D and E), providing further confirmation that the metastatic lung nodules were of endometrial origin.

Thyroid transcription factor (TTF1), is a tissue-specific transcription factor that is expressed specifically in thyroid and lung tissues (33). In the *Alk5* cKO mice, TTF1-expressing cells were detected in the normal lung tissue adjacent to the CK8-positive metastatic nodules (Fig. 5F); and as expected, only CK8-positive cells were present in the uterine tissue (Fig. 5G). Compared with controls, the uterus and lung tissue of the *Alk5* cKO mice had increased expression of the proliferation marker, Ki67 (*SI Appendix*, Fig. S4 A–D).

**Uterine Cancers and Metastatic Lung Nodules in *Alk5* cKO Mice Regress After Ovariectomy.** The majority of human endometrial tumors are categorized as type I, hormone-dependent cancers (5). After mating continuously to WT males for 3 mo to allow for tumor development, *Alk5* cKO mice were ovariectomized to determine if the endometrial tumors were hormone dependent. We first assessed the presence of lung metastases in mice continuously mated to WT males by imaging live 10-mo-old *Alk5* cKO mice with a computerized tomography (CT) scan of the chest (Fig. 6 A and B). Once lung metastases were observed, mice were either ovariectomized (OVX) or allowed to progress with intact ovaries (non-OVX). One month after ovariectomy, the chest CT was repeated in both the OVX and non-OVX mice. Whereas the presence of metastatic lung nodules was unchanged

in the non-OVX mice (Fig. 6 A and C), the lung nodules regressed in the OVX mice (Fig. 6 B and D).

Gross analysis of the uterus and lungs also showed that the endometrial cancers and metastatic lung nodules remained in the *Alk5* cKO non-OVX mice (Fig. 6 E and I). However, the lung nodules and endometrial cancers regressed in the *Alk5* cKO mice following ovariectomy (Fig. 6 F and J). Histology of the lung tissues showed regression of the tumor metastases after ovariectomy (Fig. 6 G and H). Likewise, the endometrial cancers and invasive endometrial glands were significantly reduced following ovariectomy in *Alk5* cKO mice; histology showed that most invasive glands had regressed, with fewer and smaller invasive glands remaining in the myometrium (Fig. 6 K–N). These results indicate that the maintenance of the cancers and metastatic nodules is strongly dependent on the action of ovarian hormones. However, because complete regression of invasive endometrial glands was not observed, a longer time without the presence of ovarian hormones may be required for complete regression. Alternately, other unknown factors may also contribute to endometrial cancer in these mice.

**Unilateral Oviduct Removal Demonstrates That Pregnancy Is Required for Cancer Development in *Alk5* cKO Mice.** The endometrial cancers were only observed in mice that were mated to fertile males, as virgin mice or mice mated to vasectomized males did not develop the cancer (*SI Appendix*, Table S1). As shown above, estrogen was important for maintenance of the cancer (Fig. 6); however, estrogen treatment alone was not sufficient to cause the cancers. Ovariectomized mice were treated with E2 pellets for 3 mo, and cancer did not develop in either control or *Alk5* cKO mice (*SI Appendix*, Fig. S5). To establish whether pregnancy or implantation to the uterus could lead to the cancer formation, the oviducts from one uterine horn were removed in both control and *Alk5* cKO mice followed by mating to fertile males. The female mice were dissected after 3 mo, and the uteri and lungs were examined for the presence of cancer and lung metastases,



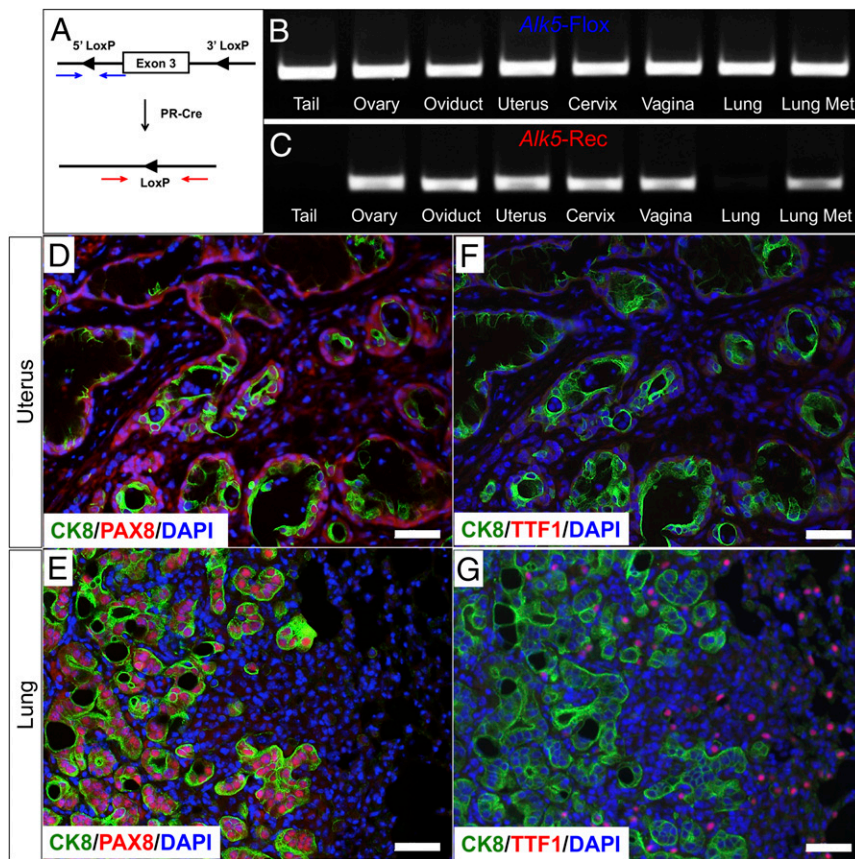


**Fig. 5.** *Alk5* cKO mice develop metastatic lung nodules that originate in the endometrium. (A) The *Alk5* allele has LoxP sites flanking exon 3. The intact LoxP sites are amplified by the primer set denoted by the blue arrows. After cre-driven recombination, the LoxP sites are amplified by the primer set indicated by the red arrows. (B and C) PCR amplification of mouse tissues from an *Alk5* cKO mouse using primers that are specific for the *Alk5* floxed allele (B) or for the recombined allele (C). (D and E) Uterine and lung sections from an *Alk5* cKO mouse stained with CK8, PAX8, and DAPI. (F and G) CK8 and TTF1 immunostaining in the uterus (F) and lung (G) tissues of *Alk5* cKO mice. Images represent tissues collected from mice that were continuously mated to WT males for 6 mo beginning at 6 wk of age. (Scale bar, 50  $\mu$ m.)

respectively. As expected, pregnancy could be detected only in the uterine horn with the intact oviduct (SI Appendix, Fig. S6 A and B). After dissection, both uterine horns (oviduct removed and oviduct intact) were normal in the control mice (Fig. 7A). In the *Alk5* cKO mice, all of the uterine horns without the oviduct were normal, but the uterine horns with the intact oviduct had cancerous masses in 8 of 13 *Alk5* cKO mice, with lung metastases observed in 4 of these *Alk5* cKO mice (Fig. 7B).

Histological analysis of the reproductive tracts showed that the uterine horns from *Alk5* cKO mice lacking the oviducts were normal, with distinct SMA-positive myometrial layers and CK8-positive epithelium (Fig. 7C and E). However, the uterine tissue from the oviduct-intact horns showed that the CK8-positive uterine glands invaded the SMA-positive myometrial compartment in the *Alk5* cKO mice (Fig. 7D and F). These results indicate that the occurrence of pregnancy or embryo implantation in the *Alk5* cKO endometrium, and not hormonal changes associated with pregnancy, results in glandular epithelial cell invasion and metastasis.

We also determined that the cancer developed in the uteri of *Alk5* cKO mice following artificial decidualization and long-term E2 treatment (SI Appendix, Fig. S7). This experiment allowed us to test whether cancer development was influenced by the implantation of the embryo to the endometrium. Control and *Alk5* cKO mice were ovariectomized and treated with 100 ng E2 and 1 mg P4 as shown in SI Appendix, Fig. S7A. On day 4 of hormonal treatments, all mice received an artificial decidual stimulus to one uterine horn, followed by E2 treatment for 3 mo. Grossly, the uterine horns from control mice were normal (SI Appendix, Fig. S7B), while the uterine horn that received the decidual stimulus in *Alk5* cKO mice developed a cancerous lesion in two of the six mice analyzed (SI Appendix, Fig. S7C). There were no significant differences between the uterine weights of control and *Alk5* cKOs in the nondecidualized ( $0.189 \pm 0.028$ ,  $0.147 \pm$

$0.009$ ,  $P = 0.364$ ) or decidualized horns ( $0.196 \pm 0.031$ ,  $0.200 \pm 0.020$ ,  $P = 0.684$ ). Cross-sections stained with smooth muscle actin and E-cadherin from the nondecidualized uterine horns, confirmed that the tissue architecture was similar between control and *Alk5* cKO mice (SI Appendix, Fig. S7D and F). However, unlike the decidualized horn of the control mice (SI Appendix, Fig. S7E), the tissue architecture was abnormal in the lesion of the decidualized horn of the *Alk5* cKO mouse (SI Appendix, Fig. S7G), showing invasion of the endometrial epithelium into the underlying myometrium. Therefore, development of the endometrial cancers in *Alk5* cKO mice required a decidual stimulus and estrogen, but not the presence of an embryo.

### Discussion

We discovered that conditional deletion of *Alk5* in the female reproductive tract resulted in endometrial cancers with metastases to the lungs. Previous studies have demonstrated that alterations in the TGF $\beta$  signaling pathway are associated with endometrial cancers. For example, analysis of endometrial tumors from a subset of women have decreased expression of phosphorylated SMAD2, TGBR1/ALK5, and TGFBR2, as well as frameshift mutations in the *TGFBR2* gene (34). Several other studies have also identified the presence of *TGFBR1* and *TGFBR2* mutations in endometrial tumors (35, 36), indicating the importance of an intact TGF $\beta$  signaling pathway for endometrial tissue homeostasis. Concentrations of the TGF $\beta$  ligands and receptors fluctuate throughout the menstrual cycle, suggesting that the TGF $\beta$  signaling pathway changes in response to steroid hormones and plays fundamental roles in the cyclic dynamic remodeling of the endometrium (37).

In addition to alterations in the TGF $\beta$  receptors, inactivating mutations in the genes encoding their downstream signaling effectors, the SMAD2, SMAD3, and SMAD4 proteins, may



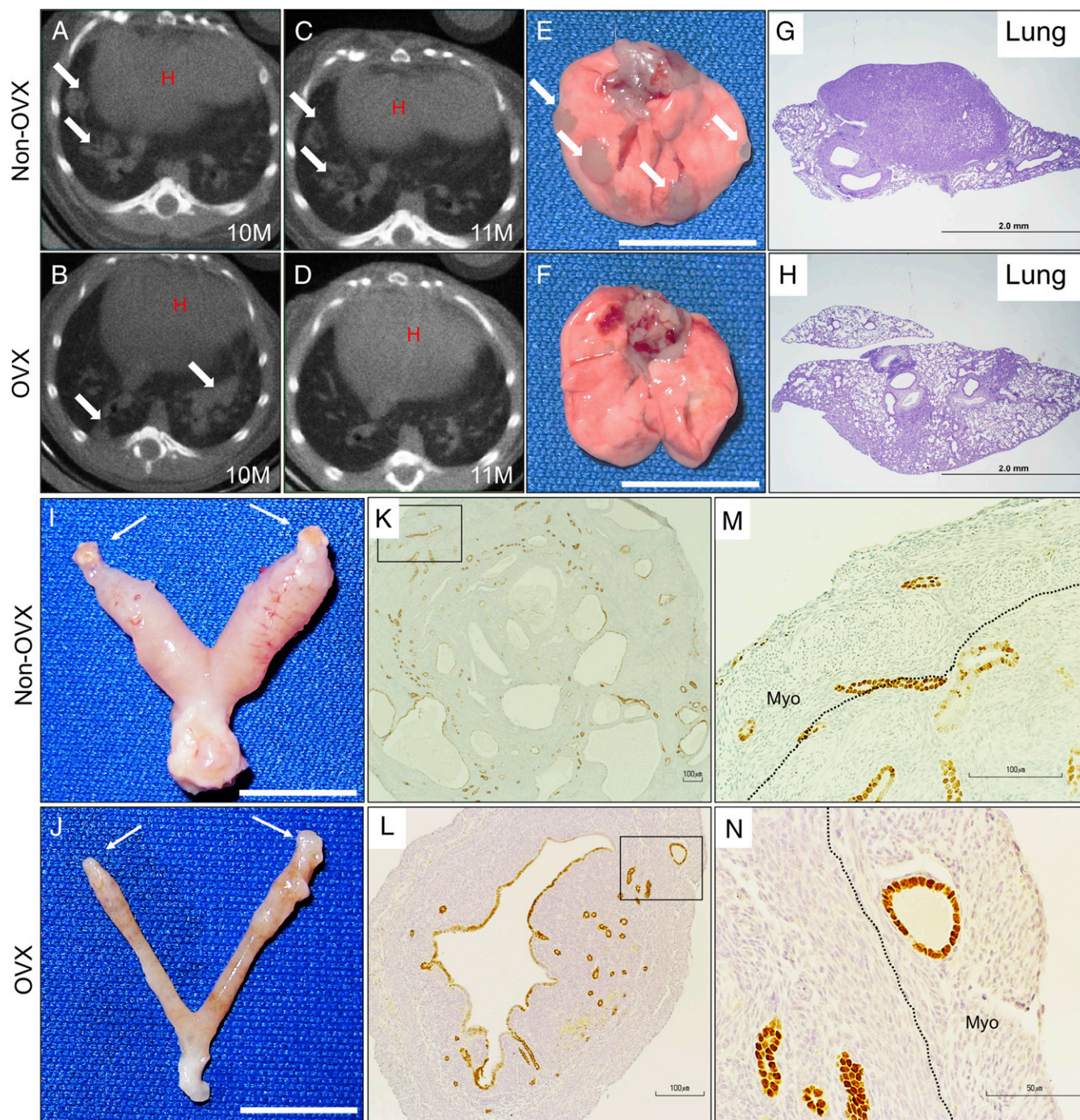


**Fig. 6.** Endometrial cancers and lung metastases in *Alk5* cKO mice regress after ovariectomy. (A and B) Chest CT scan of two 10-mo-old *Alk5* cKO mice with arrows indicating the metastatic lung nodules. (C) CT scan of the same *Alk5* cKO non-OVX mouse shown in A at 11 mo of age. (D) CT scan of the same *Alk5* cKO mouse shown in B 1 mo after OVX. (E and I) Presence of metastatic lung nodules (E) and uterine cancer (I) in an *Alk5* cKO mouse with intact ovaries (denoted by arrows). Lungs (F) and uterus (J) of an *Alk5* cKO mouse 1 mo after ovariectomy. (G and H) Lung cross-sections from an *Alk5* cKO mouse before ovariectomy (G) and 1 mo after ovariectomy (H). (K–N) FOXA2-stained cross-sections of a uterus from an *Alk5* cKO mouse with intact ovaries (K and M) and 1 mo following ovariectomy (L and N). [Scale bars, 1 cm (E, F, I, and J).]

also drive tumorigenesis. For example, mutations in the *SMAD2* and *SMAD4* genes are common in lung, colorectal, and pancreatic tumors (38–42). The role of *SMAD4* in cell cycle inhibition, mainly at the G1/S transition, places *SMAD4* as a tumor suppressor with critical roles in cell cycle control (43, 44). Therefore, a functional TGF $\beta$  signaling pathway, in which ligands, receptors, and downstream effectors function normally, is required for cell cycle control

and tumor suppression. The critical roles of TGF $\beta$  signaling are emphasized by animal models with inactivating mutations of members of this pathway. Mice with heterozygous deletion of *Smad4* develop gastric tumors and *Smad3* null mice develop aggressive metastatic rectal carcinoma (45, 46).

In the female reproductive tract, TGF $\beta$  signaling is required for development and fertility. In mice, double conditional inactivation



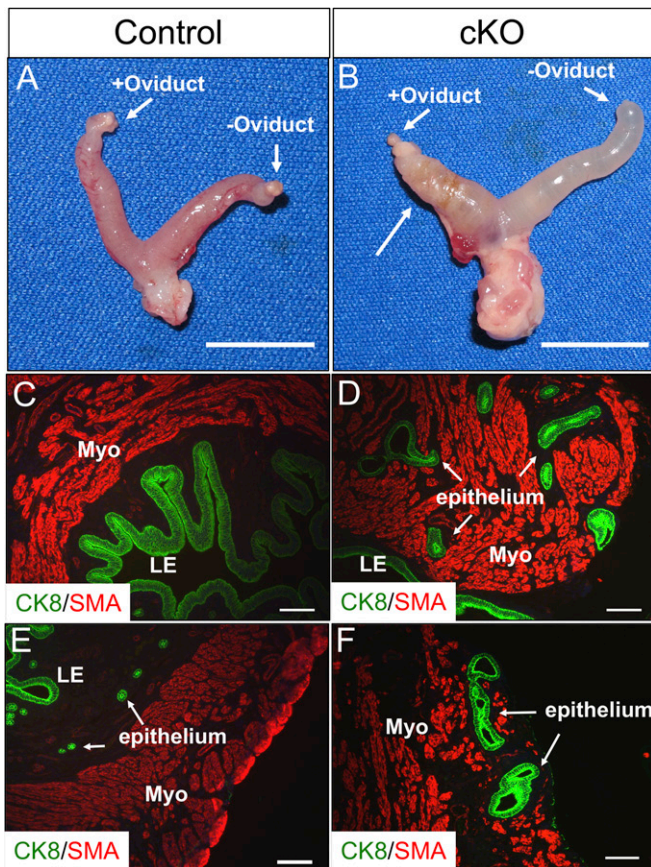


**Fig. 7.** Endometrial cancers develop in the uterine horn with an intact oviduct. (A and B) Uterus of a control (A) and *Alk5* cKO (B) mouse with a unilaterally removed oviduct. (C and E) Tissue section from the uterine horn without an oviduct from an *Alk5* cKO mouse stained with the myometrial marker, SMA, and the epithelial cell marker CK8. (D and F) Tissue section from the uterine horn with an intact oviduct from an *Alk5* cKO mouse stained with SMA and CK8. The tissues were dissected from 5-mo-old mice that were continuously mated to males for 3 mo beginning at 8 wk of age. [Scale bars, 1 cm (A and B) and 100  $\mu$ m (C–F).]

of *Smad2* and *Smad3* with *Amhr2*-cre, resulted in severe subfertility due to ovarian defects that included reduced antral follicles and decreased ovulation (47). Mice with double conditional inactivation of *PTEN* and *Tgfb1/Alk5* in the female reproductive tract with *Pgr*-cre also present aggressive endometrial tumors with metastases to the lungs (28). Since inactivating *PTEN* deletions are frequent in endometrial tumors (48), this study suggests an interplay between the two pathways in the prevention of endometrial cancer.

Unopposed estrogen action is a major risk factor for endometrial hyperplasia and endometrial cancer (49). The presence of ER $\alpha$  and PR is associated with low tumor grade and increased survival in endometrial cancer (5, 50). In the uterus, progesterone and its cognate receptor, PR, counteract the proliferative action of estrogen and ER $\alpha$  (49, 50). We identified that the endometrial tumors developed by the *Alk5* cKO mice were estrogen dependent and lost PR protein expression. Depleting the organism of ovarian steroid hormones by bilateral ovariectomy led to a significant regression of both the endometrial cancers and metastases in the *Alk5* cKO mice; however, upon closer examination the presence of invasive endometrial glands could still be detected in the myometrial compartment. This indicated that while ovarian hormones may strongly contribute to endometrial cancers and metastases in this mouse model, other unidentified factors could also contribute to the endome-

trial cancer maintenance. In women, progestin is an effective therapy for endometrial hyperplasia because it opposes estrogen action in the endometrium (49). This is also reflected in a mouse model with conditional ablation of PR in the uterine epithelium (using *Wnt7a*-cre), where the luminal uterine epithelium continues to proliferate following E2 and P4 administration (51), indicating the importance of epithelial PR in uterine function. We determined that *Alk5/Tgfb1* mRNA expression is ~10-fold higher in the luminal uterine epithelium than in the endometrial stroma and myometrial compartments, suggesting that TGF $\beta$  signaling via ALK5 is critical for uterine epithelial function. TGF $\beta$  signals through the SMAD2 and SMAD3 transcription factors; when mice are in proestrous or diestrous, *Smad3* expression is equally distributed between the epithelial and stromal/myometrial compartments of the uterus, while *Smad2* is more highly expressed in the stromal/myometrial compartments [PNAS paper by Kriseman et al. (52)]. Therefore, loss of PR protein levels in the epithelium of the *Alk5* cKO mice suggests that PR loss leads to unopposed estrogen action and endometrial cancer in the mutant mice. These findings indicate that hormone signaling and the TGF $\beta$  pathway are related and may be critical for the maintenance of endometrial function.

We observed that the *Alk5* cKO females developed endometrial, cervical, and vaginal defects when subjected to mating. *Alk5* cKO females that were mated to vasectomized males developed cervical and vaginal masses (SI Appendix, Table S1), yet endometrial cancers and lung metastases did not occur. Previous studies showed that seminal vesicle proteins that are present in both fertile and vasectomized mice trigger gene expression changes and recruit immune cells within the female reproductive tract (53, 54). Therefore, it is plausible that the inflammatory reaction elicited by proteins in the seminal fluid triggered defects in the cervical and vaginal tissues of the *Alk5* cKO mice. This is supported by the strikingly high levels of TGF $\beta$  present in seminal fluid, which trigger cytokine activation and recruit macrophages, dendritic cells, and lymphocytes to the cervical and uterine epithelium (55).

In our study, we observed that endometrial cancers and lung metastases only developed in *Alk5* cKO females that were mated to fertile males. Therefore, our study indicates that both *Tgfb1/Alk5* inactivation and endometrial transformation elicited by pregnancy were required for development of metastatic endometrial cancers. During pregnancy, the endometrium transforms into the decidua, a specialized tissue that will sustain embryo implantation and support placental development. This change is observed at the cellular level, where stromal cells differentiate into morphologically and functionally distinct decidual cells with secretory functions (56). Following parturition, stromal and epithelial cells must once again repopulate the endometrium. Postpartum endometrial regeneration is thought to occur via a stromal-to-epithelial transition, in which stromal cells of the endometrium transform into luminal epithelial cells (57). It is possible that TGF $\beta$  signaling is required for this stromal-to-epithelial transition, and the absence of *Tgfb1/Alk5* compromises the cellular differentiation program, eventually leading to cancer.

After parturition, the endometrium must undergo healing, which is characterized by a local hypoxic and inflammatory state (58). In the postpartum uterus, high levels of vascular endothelial growth factor (VEGF) and transforming growth factor  $\beta$  3 (TGF $\beta$ 3) as well as macrophages with cytoplasmic lysosomes are observed 3 d after parturition. These factors rise in response to the contractions emitted by the myometrium and are required to restore the vasculature and cellular architecture of the endometrium following the end of pregnancy. During postpartum endometrial healing, TGF $\beta$ 3 emits intracellular signals via the cell surface receptor, TGFBR1/ALK5 (58). The absence of this signaling pathway in our mouse model may partially explain why the endometrial defects that we observed in the *Alk5* cKO mice developed only after mating or after artificial decidualization. This is supported



by our previous studies, which also show that the immunologic state of the decidua and placenta during pregnancy is compromised in *Alk5* cKO mice, with decreased levels of uterine natural killer cells, cytokines, and other growth factors which are required for placental development and embryo growth (27). This study also showed that the abnormal vascular remodeling in the maternal compartment of *Alk5* cKO mice was incompatible with pregnancy and resulted in fetal loss. Future studies would be necessary to determine whether the defective vascularization at the implantation site contributes to the development of the endometrial cancer or metastases observed in the *Alk5* cKO mice.

We also tested the development of endometrial cancer in a model of artificial pregnancy followed by long-term estrogen treatment. These experimental conditions allowed us to test the development of the cancer in an environment where the endometrial epithelium regresses and the endometrial stroma differentiates similar to a natural pregnancy, but in the absence of an implanting embryo (59). Given that the mice were collected 3 mo postdecidual stimulus, we did not expect to observe the enlarged decidual horn typically seen several days following the induction (27). However, the uteri underwent decidualization, followed by endometrial repair under the influence of high estrogen levels, and therefore, we could test if the cancers developed in the absence of an embryo. We observed that cancer did develop, albeit at a low rate, indicating that the presence of an embryo does not contribute to the malignant transformation of the endometrium in *Alk5* cKO mice. The rate of cancer development observed in this experiment was low (two of six *Alk5* cKO mice), suggesting that the development of cancer may be more penetrant after exposure to repeated pregnancies. No lung metastases were detected in any of the mice.

Because the mouse model presented in this study only develops cancers in mice that are exposed to pregnancy, TGF $\beta$  signaling through TGFBR1/ALK5 must be a critical event during endometrial regeneration, and abnormal cellular signaling in the *Alk5* cKO mice may predispose the endometrium to defects during the stromal-to-epithelial cell differentiation that occurs postpartum. Because the *Alk5* cKO mice experience embryonic loss at variable developmental time points [between embryonic day 7.5 (E7.5) to E10.5], studying endometrial repair would need to be performed using an artificial model where the endometrial changes can be precisely monitored (60). Further studies are warranted to identify the relationship between endometrial regeneration, TGF $\beta$ /ALK5/TGFBR1 signaling, and the endometrial cancers that we observed in *Alk5* cKO mice.

## Materials and Methods

**Transgenic Mouse Models.** *Alk5<sup>flloxiflox</sup>* mice were a kind gift from Stefan Karlsson, Lund University, Lund, Sweden. Progesterone receptor-cre (*Pgr-cre<sup>+/+</sup>*) mice were obtained from John Lydon, Baylor College of Medicine, Houston, TX and Francesco DeMayo, National Institute of Environmental Health Sciences, Research Triangle Park, NC (31). *Alk5<sup>flloxiflox</sup>* mice were mated to *Pgr-cre<sup>+/+</sup>* mice to obtain conditional deletion of ALK5 in the PR-expressing tissues (uterus, ovary, pituitary, oviduct, vagina, and cervix). *Rosa26<sup>tdTomato</sup>* reporter mice were crossed into *Alk5<sup>flloxiflox</sup>-PRcre<sup>+/+</sup>* mice to obtain tdTomato expression in the mouse tissues with ALK5 inactivation. Mouse handling was performed in accordance with the Institutional Animal Care and Use Committee at Baylor College of Medicine. Mouse genotyping was performed as previously described (27).

**Rodent Surgeries.** All mouse surgeries were performed according to the guidelines from the Institutional Animal Care and Use Committee at Baylor College of Medicine. For the ovariectomy, mice were injected with slow release buprenorphine (ZooPharm) (1 mg/kg) and meloxicam (Norbrook) (4 mg/kg) for analgesia before surgery and up to 72 h after surgery to control pain, and anesthetized with 2% isoflurane (Piramal) with oxygen. Ovariectomy was performed by making a 0.3–0.5 cm midline incision into the skin followed by a small incision to expose the fat pad. The fat was gently pulled out of the incision and the oviduct tied with absorbable Vicryl (Ethicon) followed by cutting of the ovary with small sharp scissors. The procedure was repeated on the second ovary. The abdomen was then sutured with absorbable Vicryl, the skin, closed with a surgical clip, and the mice were

allowed to wake on a warm plate. The mice were monitored daily and injected with analgesics for a minimum of 72 h.

For long-term E2 treatment studies, mice were implanted s.c. with an estradiol-secreting pellet (0.025 mg/pellet/90 d; Innovative Research of America) 2 wk after ovariectomy. The pellets were placed for 90 d, after which the mice were killed and evaluated for cancer development.

For the unilateral oviduct removal studies, mice were anesthetized and injected as described above. After making the midline incision and exposing the fat pad, small sharp scissors were used to remove the oviduct from one uterine horn. After severing the oviduct, the uterus and ovary were left intact, and returned to the abdomen, which was sutured closed followed by skin closure with a metal surgical clip. After a 2-wk recovery period, the mice were mated to a WT male mouse for a defined period of time.

**Artificial Induction of Decidualization Followed by Long-Term E2 Treatment.** To test the effect of artificial decidualization on the development of endometrial cancers in *Alk5* cKO mice, we adapted a previously published protocol of artificial decidualization (59). Mice were ovariectomized, allowed to recover for 2 wk, and injected s.c. with 100 ng E2 for 2 d. Following 2 d of rest, mice were injected with three daily s.c. injections of 1 mg P4 plus 6.7 ng E2. On the fourth day, one uterine horn was injected with 50  $\mu$ L of sesame oil while the contralateral horn was not injected and served as a negative control. Immediately after oil injection, an estradiol-secreting pellet (0.025 mg/pellet/90 d; Innovative Research of America) was implanted s.c. into each mouse. After 3 mo, the mice were killed and the uterine horns were collected, weighed, and evaluated using histology.

**CT Scan of the Lungs.** CT was performed at the Mouse Metabolism and Phenotyping Core at Baylor College of Medicine to assess cancer progression in the *Alk5* cKO mice. CT images were taken with a Gamma Medica Flex SPEC/CT. Imaging metadata includes a pixel size of 35  $\mu$ m, matrix size is 512  $\times$  512, gantry motion was step, and binning was 2  $\times$  2. The mice were placed in the supine position and anesthetized with isoflurane during imaging. Periodic monitoring of the anesthetic level and animal well-being was performed throughout the procedure.

**Micro-CT Analysis of the Mouse Lungs.** *Alk5* cKO and control mice were fixed by perfusion using 4% paraformaldehyde. The lungs were dissected immediately after surgery and washed overnight in 1 $\times$  PBS (Invitrogen) at 4  $^{\circ}$ C. The lungs were then immersed in 0.1 N (vol/vol) iodine solution (Sigma) and incubated overnight at room temperature. The lungs were mounted in 1% (wt/vol) agarose and imaged on a SKYSCAN 1272-micro-CT scanner at the Optical Imaging and Vital Microscopy Core Facility at Baylor College of Medicine. Each sample was rotated 180 $^{\circ}$  to obtain a 3D image of the lung. The projection images were reconstructed using NRecon software as previously reported (61).

**Tissue Processing and Histology.** Tissues were fixed in 10% neutral buffered formalin (vol/vol) (VWR) overnight, then stored in 70% ethanol until embedding. Tissues were processed and embedded in paraffin at the Pathology and Histology Core at Baylor College of Medicine. Sections (5  $\mu$ m) of formalin-fixed, paraffin-embedded tissues were performed and stained with H&E (VWR).

**Antibody Immunostaining.** Formalin-fixed paraffin-embedded sections were deparaffinized with Histoclear (National Diagnostics) and rehydrated in a series of ethanol solutions. Antigen retrieval was performed in a microwave in a 10-mM citrate, 0.05% Tween-20, pH 6.0 solution. Sections were blocked in 3% BSA (Sigma) for 1 h, followed by overnight incubation in the primary antibody dissolved in 3% BSA. Detection and labeling was performed with secondary antibodies conjugated to Alexa Fluor-488 or Alexa Fluor-594 (Invitrogen) fluorophores and imaged using an Olympus BX51 fluorescence microscope. All antibodies and dilutions are listed in *SI Appendix, Table S2*.

**ACKNOWLEDGMENTS.** We thank Drs. John Lydon and Francesco DeMayo for providing the *PRcre* mouse line, Dr. Stefan Karlsson for providing the *Alk5<sup>flloxiflox</sup>* mouse line, and Dr. Donna M. Coffey (Houston Methodist Hospital) for her analysis of the uterine histology. These studies were supported by Eunice Kennedy Shriver National Institute of Child Health and Human Development Grants R01-HD032067 and R01-HD033438 (to M.M.M.), K99-HD096057 (to D.M.), the Institutional Research and Academic Career Development Award K12-GM084897 (to D.M.), the New Jersey Commission on Cancer Research Fellowship (to J.P.), the Brewster Foundation (Y.K.), and National Institutes of Health Grant R01-CA212410 (to Y.K.). D.M. holds a Postdoctoral Enrichment Program Award from the Burroughs Wellcome Fund. CT analysis of the mice was performed in the Mouse Metabolism and Phenotyping Core at Baylor College of Medicine with funding from National Institutes of Health Grants UM1HG006348 and R01DK114356.



1. Siegel RL, Miller KD, Jemal A (2017) Cancer statistics, 2017. *CA Cancer J Clin* 67:7–30.
2. Amant F, et al. (2005) Endometrial cancer. *Lancet* 366:491–505.
3. Lortet-Tieulent J, Ferlay J, Bray F, Jemal A (2017) International patterns and trends in endometrial cancer incidence, 1978–2013. *J Natl Cancer Inst* 110:354–361.
4. Lax SF, Kurman RJ (1997) A dualistic model for endometrial carcinogenesis based on immunohistochemical and molecular genetic analyses. *Verh Dtsch Ges Pathol* 81:228–232.
5. Bokhman JV (1983) Two pathogenetic types of endometrial carcinoma. *Gynecol Oncol* 15:10–17.
6. Byron SA, et al. (2012) FGFR2 point mutations in 466 endometrioid endometrial tumors: Relationship with MSI, KRAS, PIK3CA, CTNNB1 mutations and clinicopathological features. *PLoS One* 7:e38081.
7. Cheung LW, et al. (2011) High frequency of PIK3R1 and PIK3R2 mutations in endometrial cancer elucidates a novel mechanism for regulation of PTEN protein stability. *Cancer Discov* 1:170–185.
8. Salvesen HB, et al. (2009) Integrated genomic profiling of endometrial carcinoma associates aggressive tumors with indicators of PI3 kinase activation. *Proc Natl Acad Sci USA* 106:4834–4839.
9. Kuhn E, et al. (2012) Identification of molecular pathway aberrations in uterine serous carcinoma by genome-wide analyses. *J Natl Cancer Inst* 104:1503–1513.
10. Le Gallo M, et al.; NIH Intramural Sequencing Center (NISC) Comparative Sequencing Program (2012) Exome sequencing of serous endometrial tumors identifies recurrent somatic mutations in chromatin-remodeling and ubiquitin ligase complex genes. *Nat Genet* 44:1310–1315.
11. Kandoth C, et al.; Cancer Genome Atlas Research Network (2013) Integrated genomic characterization of endometrial carcinoma. *Nature* 497:67–73.
12. Miyazono K (2000) Positive and negative regulation of TGF-beta signaling. *J Cell Sci* 113:1101–1109.
13. Derynck RMK (2008) *TGF-B and the TGF-B Family* (Cold Spring Harbor Lab Press, Cold Spring Harbor, NY).
14. Miyazono K (2000) TGF-beta signaling by Smad proteins. *Cytokine Growth Factor Rev* 11:15–22.
15. Greenman C, et al. (2007) Patterns of somatic mutation in human cancer genomes. *Nature* 446:153–158.
16. Wang D, et al. (2000) Analysis of specific gene mutations in the transforming growth factor-beta signal transduction pathway in human ovarian cancer. *Cancer Res* 60:4507–4512.
17. Wang D, et al. (1997) Mutation and downregulation of the transforming growth factor beta type II receptor gene in primary squamous cell carcinomas of the head and neck. *Carcinogenesis* 18:2285–2290.
18. Massagué J (2008) TGFbeta in cancer. *Cell* 134:215–230.
19. Levy L, Hill CS (2006) Alterations in components of the TGF-beta superfamily signaling pathways in human cancer. *Cytokine Growth Factor Rev* 17:41–58.
20. Markowitz S, et al. (1995) Inactivation of the type II TGF-beta receptor in colon cancer cells with microsatellite instability. *Science* 268:1336–1338.
21. Tanaka S, Mori M, Mafune K, Ohno S, Sugimachi K (2000) A dominant negative mutation of transforming growth factor-beta receptor type II gene in microsatellite stable oesophageal carcinoma. *Br J Cancer* 82:1557–1560.
22. Monsivais D, Matzuk MM, Pangas SA (2017) The TGF-β family in the reproductive tract. *Cold Spring Harb Perspect Biol* 9:a022251.
23. Jamin SP, Arango NA, Mishina Y, Hanks MC, Behringer RR (2002) Requirement of Bmpr1a for Müllerian duct regression during male sexual development. *Nat Genet* 32:408–410.
24. Mishina Y, Hanks MC, Miura S, Tallquist MD, Behringer RR (2002) Generation of Bmpr/Alk3 conditional knockout mice. *Genesis* 32:69–72.
25. Rodriguez A, et al. (2016) SMAD signaling is required for structural integrity of the female reproductive tract and uterine function during early pregnancy in mice. *Biol Reprod* 95:44.
26. Li Q, et al. (2011) Transforming growth factor β receptor type 1 is essential for female reproductive tract integrity and function. *PLoS Genet* 7:e1002320.
27. Peng J, et al. (2015) Uterine activin receptor-like kinase 5 is crucial for blastocyst implantation and placental development. *Proc Natl Acad Sci USA* 112:E5098–E5107.
28. Gao Y, Lin P, Lydon JP, Li Q (2017) Conditional abrogation of transforming growth factor-β receptor 1 in PTEN-inactivated endometrium promotes endometrial cancer progression in mice. *J Pathol* 243:89–99.
29. Arbeit JM, Howley PM, Hanahan D (1996) Chronic estrogen-induced cervical and vaginal squamous carcinogenesis in human papillomavirus type 16 transgenic mice. *Proc Natl Acad Sci USA* 93:2930–2935.
30. Karnezis AN, et al. (2017) Evaluation of endometrial carcinoma prognostic immunohistochemistry markers in the context of molecular classification. *J Pathol Clin Res* 3:279–293.
31. Soyay SM, et al. (2005) Cre-mediated recombination in cell lineages that express the progesterone receptor. *Genesis* 41:58–66.
32. Yemelyanova A, et al. (2014) PAX8 expression in uterine adenocarcinomas and mesonephric proliferations. *Int J Gynecol Pathol* 33:492–499.
33. Lazzaro D, Price M, de Felice M, Di Lauro R (1991) The transcription factor TTF-1 is expressed at the onset of thyroid and lung morphogenesis and in restricted regions of the foetal brain. *Development* 113:1093–1104.
34. Parekh TV, et al. (2002) Transforming growth factor beta signaling is disabled early in human endometrial carcinogenesis concomitant with loss of growth inhibition. *Cancer Res* 62:2778–2790.
35. Piestrzeniewicz-Ulanska D, Brys M, Semczuk A, Jakowicki JA, Krajewska WM (2002) Expression of TGF-beta type I and II receptors in normal and cancerous human endometrium. *Cancer Lett* 186:231–239.
36. Sakaguchi J, et al. (2005) Aberrant expression and mutations of TGF-beta receptor type II gene in endometrial cancer. *Gynecol Oncol* 98:427–433.
37. Godkin JD, Doré JJ (1998) Transforming growth factor beta and the endometrium. *Rev Reprod* 3:1–6.
38. Fullerton PT, Jr, Creighton CJ, Matzuk MM (2015) Insights into SMAD4 loss in pancreatic cancer from inducible restoration of TGF-β signaling. *Mol Endocrinol* 29:1440–1453.
39. Hahn SA, et al. (1996) DPC4, a candidate tumor suppressor gene at human chromosome 18q21.1. *Science* 271:350–353.
40. Riggins GJ, Kinzler KW, Vogelstein B, Thiagalingam S (1997) Frequency of Smad gene mutations in human cancers. *Cancer Res* 57:2578–2580.
41. Yanagisawa K, et al. (2000) Heterogeneities in the biological and biochemical functions of Smad2 and Smad4 mutants naturally occurring in human lung cancers. *Oncogene* 19:2305–2311.
42. Zhao M, Mishra L, Deng CX (2018) The role of TGF-β/SMAD4 signaling in cancer. *Int J Biol Sci* 14:111–123.
43. Massagué J, Blain SW, Lo RS (2000) TGFbeta signaling in growth control, cancer, and heritable disorders. *Cell* 103:295–309.
44. Hannon GJ, Beach D (1994) p15INK4B is a potential effector of TGF-beta-induced cell cycle arrest. *Nature* 371:257–261.
45. Zhu Y, Richardson JA, Parada LF, Graff JM (1998) Smad3 mutant mice develop metastatic colorectal cancer. *Cell* 94:703–714.
46. Xu X, et al. (2000) Haploid loss of the tumor suppressor Smad4/Dpc4 initiates gastric polyposis and cancer in mice. *Oncogene* 19:1868–1874.
47. Li Q, et al. (2008) Redundant roles of SMAD2 and SMAD3 in ovarian granulosa cells in vivo. *Mol Cell Biol* 28:7001–7011.
48. Tashiro H, et al. (1997) Mutations in PTEN are frequent in endometrial carcinoma but rare in other common gynecological malignancies. *Cancer Res* 57:3935–3940.
49. Kim JJ, Chapman-Davis E (2010) Role of progesterone in endometrial cancer. *Semin Reprod Med* 28:81–90.
50. Weiderpass E, et al. (1999) Risk of endometrial cancer following estrogen replacement with and without progestins. *J Natl Cancer Inst* 91:1131–1137.
51. Franco HL, et al. (2012) Epithelial progesterone receptor exhibits pleiotropic roles in uterine development and function. *FASEB J* 26:1218–1227.
52. Kriseman M, et al. (2019) Uterine double-conditional inactivation of Smad2 and Smad3 in mice causes endometrial dysregulation, infertility, and uterine cancer. *Proc Natl Acad Sci USA* 116:3873–3882.
53. Robertson SA, Mau VJ, Tremellen KP, Seamark RF (1996) Role of high molecular weight seminal vesicle proteins in eliciting the uterine inflammatory response to semen in mice. *J Reprod Fertil* 107:265–277.
54. Robertson SA, Sharkey DJ (2016) Seminal fluid and fertility in women. *Fertil Steril* 106:511–519.
55. Robertson SA, Ingman WV, O'Leary S, Sharkey DJ, Tremellen KP (2002) Transforming growth factor beta-A mediator of immune deviation in seminal plasma. *J Reprod Immunol* 57:109–128.
56. Gellersen B, Brosens IA, Brosens JJ (2007) Decidualization of the human endometrium: Mechanisms, functions, and clinical perspectives. *Semin Reprod Med* 25:445–453.
57. Huang CC, Orvis GD, Wang Y, Behringer RR (2012) Stromal-to-epithelial transition during postpartum endometrial regeneration. *PLoS One* 7:e44285.
58. Yoshii A, Kitahara S, Ueta H, Matsuno K, Ezaki T (2014) Role of uterine contraction in regeneration of the murine postpartum endometrium. *Biol Reprod* 91:32.
59. Finn CA, Martin L (1972) Endocrine control of the timing of endometrial sensitivity to a decidual stimulus. *Biol Reprod* 7:82–86.
60. Cousins FL, et al. (2014) Evidence from a mouse model that epithelial cell migration and mesenchymal-epithelial transition contribute to rapid restoration of uterine tissue integrity during menstruation. *PLoS One* 9:e86378.
61. Hsu CW, et al. (2016) Three-dimensional microCT imaging of mouse development from early post-implantation to early postnatal stages. *Dev Biol* 419:229–236.